

See discussions, stats, and author profiles for this publication at: <https://www.researchgate.net/publication/257705926>

Water-Soluble Phosphanes Derived from 1,3,5-Triaza-7-phosphaadamantane and Their Reactivity towards Gold(I) Complexes

ARTICLE *in* EUROPEAN JOURNAL OF INORGANIC CHEMISTRY · APRIL 2013

Impact Factor: 2.94 · DOI: 10.1002/ejic.201201411

CITATIONS

9

READS

32

5 AUTHORS, INCLUDING:



Elena Cerrada

University of Zaragoza.

85 PUBLICATIONS 971 CITATIONS

SEE PROFILE

DOI:10.1002/ejic.201201411

Water-Soluble Phosphanes Derived from 1,3,5-Triaza-7-phosphaadamantane and Their Reactivity towards Gold(I) Complexes

Elena García-Moreno,^[a] Elena Cerrada,^[a] M. José Bolsa,^[a] Asunción Luquin,^[a] and Mariano Laguna^{*[a]}

Keywords: Phosphanes / Gold / Water solubility / Cytotoxicity

New water-soluble phosphanes derived from 1,3,5-triaza-7-phosphaadamantane, namely, [PTA-R]Br (R = -CH₂C≡CH, -CH₂CONH₂, -CH₂COOH), are described. Coordination of these phosphanes and their previously reported counterparts (R = -CH₂CN, -CH₂Ph and -CH₂COOMe) to gold(I) salts gives water-soluble derivatives with chlorido, bromido or pentafluorophenyl coligands. The luminescence properties of all new compounds have been studied in the solid state and compared with the respective free PTA ligands. [PTA-

CH₂Ph]Br, [PTA-CH₂COOMe]Br and [AuBr(PTA-CH₂Ph)]Br have also been characterised by X-ray diffraction analysis. Some of the new gold(I) compounds exhibit strong antiproliferative effects in the human ovarian carcinoma cell line A2780 and its cisplatin-resistant variant (A2780cisR). A balanced relationship between lipophilicity and hydrophilicity is found in these derivatives, with distribution coefficients (log *D*_{7,4}) that range from 0.14 to -0.40.

Introduction

Water is the ideal solvent for synthetic processes from an economical and ecological industrial point of view. Furthermore, as water is abundant and environmentally benign, it can be considered to be an important solvent for industrial biphasic processes.^[1–3] However, the use of water as a solvent requires the synthesis of reagents that are both stable and soluble in this medium. One of the most common strategies for solubilising metallic derivatives in water involves the use of ligands with hydrophilic properties. Amongst the many water-soluble phosphanes currently available, the adamantane-like phosphane 1,3,5-triaza-7-phosphaadamantane (PTA) has received special attention owing to its similar reactivity to other alkylphosphanes and its higher air stability and higher resistance to oxidation than other water-soluble phosphanes.^[4,5] As a result, many examples of complexes with PTA and its derivatives are known and have been reviewed recently.^[6,7]

Similar or even higher water solubilities can be achieved by *N*-alkylating PTA to form [PTA-R]X derivatives [R = Me,^[8–10] Et,^[11] *n*Pr,^[12] *n*Bu,^[12] (CH₂)₄I,^[13] CH₂Ph^[14,15] and CH₂Py^[16] (Py = pyridine)]. In addition to these alkyl salts, which are normally obtained in acetone or methanol under

reflux conditions, new alkylated PTA phosphanes, for example, [PTA-CH₂CN]Br, [PTA-CH₂Ph]Br and [PTA-CH₂COOMe]X (X = Br, OTf, PF₆) have been obtained by some of us^[17] under milder conditions. Indeed in the particular case of the ester derivative with bromine, such phosphanes have considerably higher water solubility (up to 6 times higher than PTA itself). Double *N*-alkylation of the PTA molecule, which has only been obtained with methyl groups to date, gives *N,N'*-dimethyl-1,3,5-triaza-7-phosphaadamantane^[18] {dmPTA}(CF₃SO₃)₂, which, in the presence of KOH, leads to the new water-soluble phosphane dmoPTA upon elimination of the CH₂ group between the two N-Me units.^[19] Removal of two methylene groups after the triple alkylation of tetrakis(hydroxymethyl)phosphonium chloride (THPC) leads to [P(CH₂NH₂R){CH₂N(R)CH₂N(R)CH₂}]⁺ (R = C₆H₅CH₂, 4-FC₆H₅CH₂), in which the presence of intramolecular hydrogen bonding preserves the adamantane core.^[20]

Phosphanes are some of the most frequently employed ligands in organometallic and coordination chemistry, and many of the properties that make phosphane complexes attractive for use in catalysis are also relevant for medicinal applications. In the synthesis of metal-based drugs, for example, the reactivity of the complex must be taken into account to prevent undesirable side reactions whilst allowing binding to cellular targets by ligand substitution. Furthermore, a balance between hydrophilicity and lipophilicity is required for the drug to be water soluble and at the same time be able to pass through the phospholipid cell membrane.^[21–24]

[a] Departamento de Química Inorgánica, Instituto de Síntesis Química y Catálisis Homogénea, Universidad de Zaragoza – C.S.I.C.
50009 Zaragoza, Spain
Fax: +34-976-761187
E-mail: mlaguna@unizar.es
Homepage: <http://www.unizar.es/icma/depart/qoa/web/index.php>

The earliest example of a metal–phosphane derivative with medical applications is the gold(I) complex known as auranofin [(1-thio-β-D-glucopyranose-2,3,4,6-tetraacetato-*S*)(triethylphosphane)gold], which exhibits antiarthritic properties^[25] and has also been found to be cytotoxic towards leukaemia cells.^[26,27] Recent examples of water-soluble metal–phosphane derivatives with anticancer properties towards different cell lines have also been published. Indeed, in the particular case of gold(I)^[28–32] and ruthenium(II)^[22,33–39] complexes, the presence of the hydrophilic phosphane PTA provides water solubility to these compounds.

In light of this, herein we report the synthesis of several new hydrophilic phosphanes derived from the PTA molecule, which in some cases display higher water solubility than PTA itself, and their corresponding phosphane–gold(I) derivatives. The cytotoxic properties of some of them against human ovarian carcinoma cell lines (A2780 and A2780cisR) are also reported and compared with those of cisplatin.

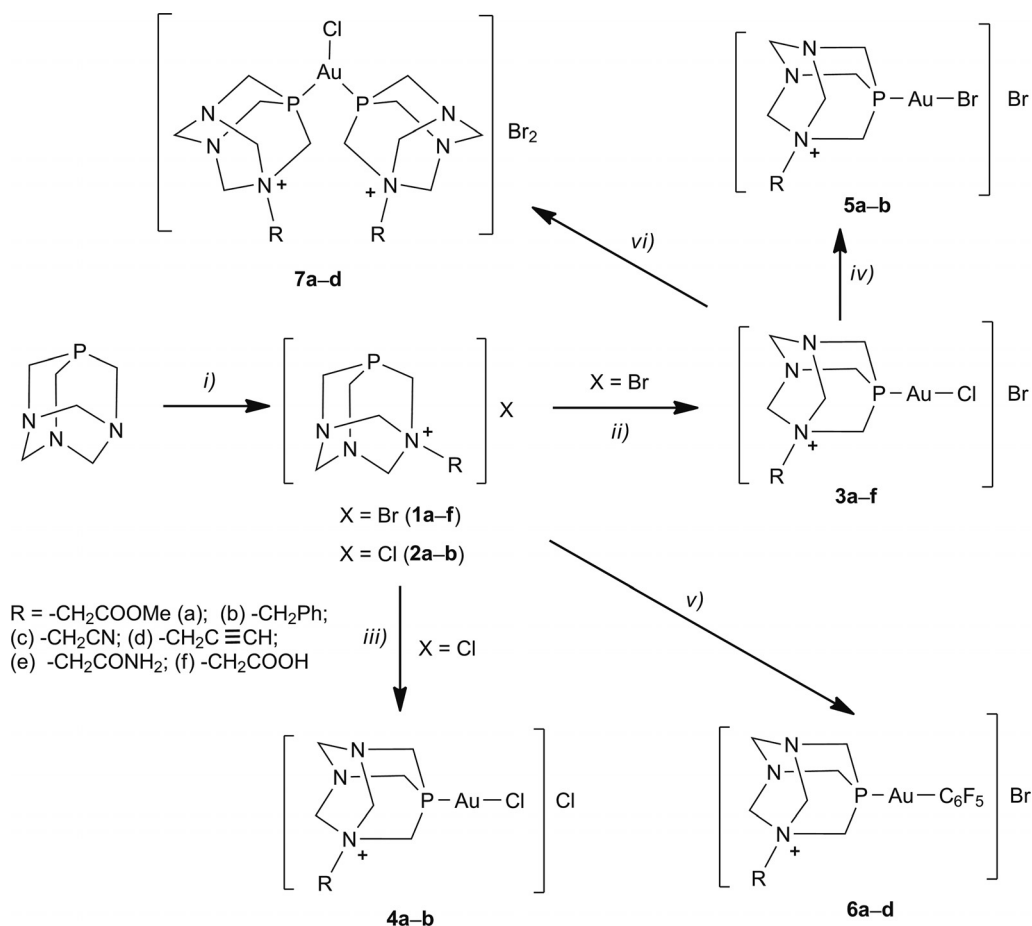
Results and Discussion

The new *N*-alkylated PTA phosphanes were prepared as described previously^[17] by treating PTA with the ap-

propriate RBr salt ($R = -CH_2C\equiv CH$, $-CH_2CONH_2$, $-CH_2COOH$), at room temperature (Scheme 1, i), to give white, water-soluble and air-stable solids. As was the case for the previously reported *N*-substituted PTA derivatives, the 1H NMR spectra of the water-soluble phosphanes are rather more complicated than that for PTA since alkylation of one of the N atoms reduces the symmetry in the molecule. Consequently, the methylene protons are inequivalent and, in some cases, diastereotopic. The methylene NCH_2N protons in all these phosphanes are diastereotopic, although the methylene protons of the NCH_2N^+ group with one alkylated N atom appear as an AB system. The $^{31}P\{^1H\}$ NMR spectra display a singlet in the range between $\delta = -81$ and -84 ppm, downfield from that for free PTA. These new phosphanes are water soluble and, in the particular case of [PTA- CH_2CONH_2] (**1e**) and [PTA- CH_2COOH] (**1f**), the solubility is two and even three times higher than that of PTA.

Treatment of these phosphanes with [AuCl(tht)] (tht = tetrahydrothiophene) leads to the formation of [AuCl(PTA-*R*)]Br derivatives as a result of replacement of the tht ligand by PTA-*R* (Scheme 1, ii).

Coordination of the Au-*L* fragment markedly affects the 1H NMR spectra, with only the AB system corresponding to the methylene NCH_2N^+ protons remaining at a similar



Scheme 1. (i) RX , (ii, iii) $[AuCl(tht)]$, (iv) $NaBr$, (v) $[Au(C_6F_5)(tht)]$ and (vi) $[PTA-R]X$.

chemical shift. The remaining protons appear as multiplets resulting from overlapping doublets and, in general, are displaced to high field with respect to those of the free phosphanes. All complexes show singlet resonances at about $\delta = -30$ ppm in their $^{31}\text{P}\{^1\text{H}\}$ NMR spectra, with the exception of **3c** that appears at $\delta = -75$ ppm, with these signals being displaced to lower field with respect to those for the corresponding free phosphanes.

Molecular peaks are observed in the MALDI+ mass spectra of all compounds, with additional peaks assigned to species in which the chlorine anion has been replaced by a bromine counterion also being detected for some of the gold(I) derivatives. This latter observation suggests a fast interchange between both anions in solution and probably means that a mixture of both salts is present in the complexes. A similar behaviour is also observed in pentafluorophenyl gold(I) complexes of related PTA ligands $[\text{Au}(\text{C}_6\text{F}_5)(\text{PTA}-\text{R})]\text{Br}$ (**6a–d**), which are prepared in a similar way but starting from $[\text{Au}(\text{C}_6\text{F}_5)(\text{tht})]$ (Scheme 1, v).

This anion exchange can be avoided by starting from the corresponding PTA chloride salt. Thus, we have prepared the PTA salts $[\text{PTA}-\text{R}]\text{Cl}$ (see the Exp. Sect.), which require longer reaction times and higher reaction temperatures. No significant differences were found in either the ^1H or $^{31}\text{P}\{^1\text{H}\}$ NMR spectra of these latter compounds with respect to their bromine-containing counterparts. However, the corresponding gold(I) derivatives of the type $[\text{AuCl}(\text{PTA}-\text{R})]\text{Cl}$ (**4a,b**; Scheme 1, iii) show some differences in their ^1H NMR spectra: for example, a displacement of the AB system that corresponds to the NCH_2N group or a greater separation between the signals of the NCH_2P , NCH_2N and CH_2X groups, thus allowing them to be more easily assigned. Surprisingly, the solubility of $[\text{PTA}-\text{CH}_2\text{CO}_2\text{Me}]\text{Cl}$ (2586 g L^{-1}) is twice that of the corresponding bromine salt $[\text{PTA}-\text{CH}_2\text{CO}_2\text{Me}]\text{Br}$ (1450 g L^{-1})^[17] and 11 times higher than that of PTA, although the gold(I) complex $[\text{AuCl}(\text{PTA}-\text{CH}_2\text{CO}_2\text{Me})]\text{Cl}$ is less soluble than the related complex $[\text{AuCl}(\text{PTA}-\text{CH}_2\text{CO}_2\text{Me})]\text{Br}$ (see the Exp. Sect.).

Substitution of the chlorine linked to gold(I) by bromine also affords pure derivatives with the formula $[\text{AuBr}(\text{PTA}-\text{R})]\text{Br}$ (**5a,b**), which can be isolated in essentially quantitative yield upon treatment of $[\text{AuCl}(\text{PTA}-\text{R})]\text{Br}$ (**3a,b**) with an excess amount of NaBr. In this case, the main differences are found in the displacement of the resonances in the $^{31}\text{P}\{^1\text{H}\}$ NMR spectra to low field by about $\delta = 10$ ppm.

Addition of a second molecule of $[\text{PTA}-\text{R}]\text{X}$ ($\text{X} = \text{Cl}, \text{Br}$) to the gold(I) chloride derivatives $[\text{AuCl}(\text{PTA}-\text{R})]\text{X}$ gives rise to $[\text{AuCl}(\text{PTA}-\text{R}_2)]\text{X}_2$, which contains two phosphanes coordinated to the Au–Cl unit, most probably in a trigonal disposition.

All gold complexes except **3b** and **4b** are water soluble, although, as expected, less so than the free phosphanes, with values that range from 4 to around 240 g L^{-1} at room temperature. The most water-soluble derivatives are those that contain the PTA phosphane with an ester or amide group, which are also the most soluble phosphanes. A slight increase in water solubility is observed in derivatives **7b–d**, which contain two phosphanes per molecule with respect to their precursors **3b–d**.

Some of these derivatives are luminescent at room temperature and at 77 K in the solid state (Table 1). As an example, the emission of $[\text{AuCl}(\text{PTA}-\text{CH}_2\text{CO}_2\text{Me})]\text{Br}$ (**3c**) is plotted in Figure 1.

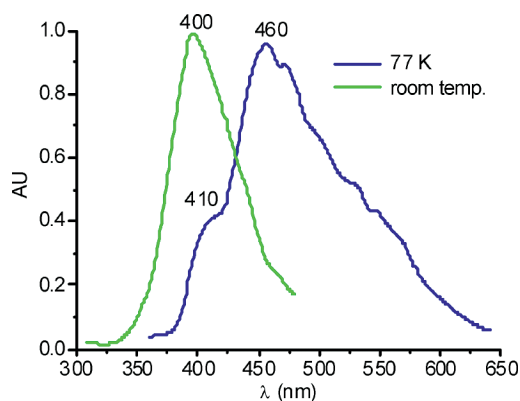


Figure 1. Emission spectra of $[\text{AuCl}(\text{PTA}-\text{CH}_2\text{CO}_2\text{Me})]\text{Br}$ (**3a**) at room temperature (green) and (blue) at 77 K.

Table 1. Excitation and emission data in the solid state.^[a]

	298 K		77 K	
	λ_{exc} [nm]	λ_{emis} [nm]	λ_{exc} [nm]	λ_{emis} [nm]
$[\text{PTA}-\text{CH}_2\text{CO}_2\text{Me}]\text{Br}$ (1a)	–	–	380	440
$[\text{PTA}-\text{CH}_2\text{Ph}]\text{Br}$ (1b)	–	–	280	400 (sh), 440
$[\text{PTA}-\text{CH}_2\text{CN}]\text{Br}$ (1c)	–	–	–	–
$[\text{AuCl}(\text{PTA}-\text{CH}_2\text{CO}_2\text{Me})]\text{Br}$ (3a)	370	415 (sh), 440	340	400 (sh), 450
$[\text{AuCl}(\text{PTA}-\text{CH}_2\text{Ph})]\text{Br}$ (3b)	360	400 (sh), 450	355	460
$[\text{AuCl}(\text{PTA}-\text{CH}_2\text{CN})]\text{Br}$ (3c)	315	400	340	460 (st)
$[\text{AuCl}(\text{PTA}-\text{CH}_2\text{CO}_2\text{Me})]\text{Cl}$ (4a)	380	430, 450	340(st)	440 (st)
$[\text{AuCl}(\text{PTA}-\text{CH}_2\text{Ph})]\text{Cl}$ (4b)	–	–	340	445 (st)
$[\text{AuBr}(\text{PTA}-\text{CH}_2\text{CO}_2\text{Me})]\text{Br}$ (5a)	290	520	287, 350	455 (sh), 495
$[\text{AuBr}(\text{PTA}-\text{CH}_2\text{Ph})]\text{Br}$ (5b)	320	550	346	450, 550
$[\text{Au}(\text{C}_6\text{F}_5)(\text{PTA}-\text{CH}_2\text{CO}_2\text{Me})]\text{Br}$ (6a)	–	–	300	530
$[\text{Au}(\text{C}_6\text{F}_5)(\text{PTA}-\text{CH}_2\text{Ph})]\text{Br}$ (6b)	380	480	360	470
$[\text{Au}(\text{C}_6\text{F}_5)(\text{PTA}-\text{CH}_2\text{C}\equiv\text{CH})]\text{Br}$ (6d)	320	370	330, 340 (sh)	460, 550

[a] sh: shoulder, st: structured band.

The *N*-alkylated phosphanes are not luminescent at room temperature and exhibit a weak luminescence at 77 K, but after coordination to gold(I), most of the obtained complexes are luminescent even at room temperature. Complexes **3a–c**, **4a,b** and **6a–c** show an emission band between 400 and 460 nm, however, complexes **5a,b** show lower-energy bands, around 500 nm, which could be in accordance with the assignment of ligand-to-metal charge transfer (LMCT) nature of this emission. This assignment is supported by the crystal structure of [AuBr(PTA-CH₂Ph)]Br (**5b**), described here (see below). This structure contains dimers with shorter Au...Au distances than the previously reported PTA derivative.

At 77 K the behaviour is similar for all the complexes that show maxima between 400 and 460 nm. Complexes **4a,b** show structured bands with intensity maxima about 440 nm and complex **6a** shows an emission maximum about 530 nm. Emissions observed at room temperature and at 77 K for all complexes are similar to those observed for the free phosphanes **1a–c** at 77 K, which could suggest an origin for the emission: intraligand perturbed by the metal or a band mixture of intraligand and ligand-to-metal-centred. The related derivatives [AuCl(PTA)] and [AuBr(PTA)], and the corresponding protonated complexes [AuCl(PTA-H)]Cl and [AuBr(PTA-H)]Br, also show photoluminescent behaviour, with strong temperature-dependent emissions assigned to LMCTs.^[40,41]

Structural Results

The X-ray structure of [PTA-CH₂CO₂Me]⁺ with triflate (CF₃SO₃) as counteranion has been described previously.^[17] The molecule presents disorder in the phosphorus and one of the nitrogen atoms, with the respective positions being interchanged in the cation. This leads to atypical P–C and N–C distances, some 0.25 Å shorter or longer, respectively, than conventional values. Herein we describe the crystal structure of the water solvate of [PTA-CH₂CO₂Me]Br (**1a**), which does not have the symmetry problems found in [PTA-CH₂CO₂Me](CF₃SO₃). The methanol solvate of [PTA-CH₂Ph]Br (**1b**) has also been characterised by X-ray diffraction. These molecules are depicted in Figures 2 and 3, with selected bond lengths and angles in Tables 2 and 3, respectively. The bond angle around the phosphorus atom (C–P1–C = 96.23° in **1b** and 96.21° in **1a**, on average) displays a distorted-pyramidal geometry similar to that observed in free PTA^[42] or in the related PTA derivatives [pymePTA]Br (pyme = *N*-methylpyridinium),^[16] [PTA-(CH₂)₄I]I,^[13] [PTA-1-allyl]I^[43] and [dmPTA](CF₃SO₃)₂.^[18] Larger C–P–C angles (97.78–99.42°) are found in [P(CH₂NH₂R){CH₂N(R)CH₂N(R)CH₂}X (R = C₆H₅CH₂, 4-FC₆H₅CH₂; X = Cl and SbF₆),^[20] in which the adamantane core is maintained by means of intramolecular hydrogen bonds. The geometry around N2 and N3 is also distorted pyramidal, with average C–N–C angles of 111.13(2) and 111.33(2)° for **1b** and 111.18 and 111.53° for **3**, respectively. However, the quaternary N1 atom shows a nearly

ideal tetrahedral geometry, with average C–N–C angles of 109.0(2)° in **1b** and 109.42° in **3** (see Table 4). As is the case for the previously reported PTA derivatives [pymePTA]Br, [PTA-(CH₂)₄I]I and [dmPTA](TfO)₂, the average N–C bond lengths [1.526(3) (**1b**) and 1.527(3) Å (**1a**)] for this quaternary N atom are slightly longer than that observed around N2 [1.456(4) (**1b**) and 1.454(3) Å (**1a**)] and N3 [1.460(4) (**1b**) and 1.456(3) Å (**1a**)]. In the case of [PTA-CH₂CO₂Me]Br (**1a**), the oxygen atom of the ketone group (O1) displays short intramolecular O1...N1 contacts of 2.899(3) Å and additional intramolecular C–H...O interactions [C9–H9C...O1 2.35 Å, C9...O3 2.708(3) Å and angle at H9C of 101°; C3–H3B...O1 2.46 Å, C3...O1 3.088(3) Å and angle at H3B of 120°]. The molecules pack in groups of three molecules interconnected through short P...N distances of 3.394(2) Å. Additionally, the unit cell of **1b** shows that the packing of individual cations is influenced by very

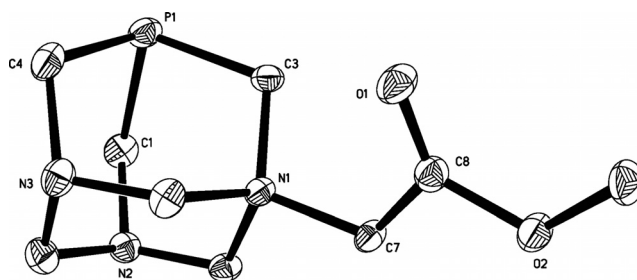


Figure 2. ORTEP plot showing the X-ray structure of the cation in [PTA-CH₂CO₂Me]Br (**1a**). Thermal ellipsoids are drawn at 50% probability. Hydrogen atoms are omitted for clarity.

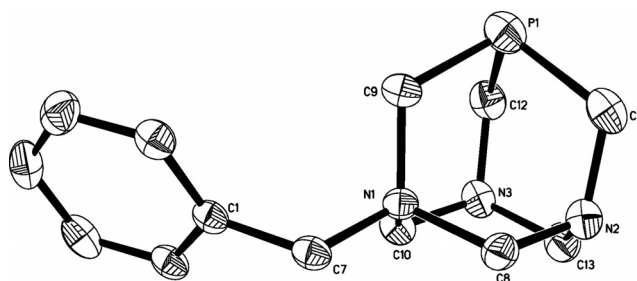


Figure 3. Molecular structure of [PTA-CH₂Ph]Br (**1b**) showing the cation. Thermal ellipsoids are drawn at the 50% probability level. Hydrogen atoms are omitted for clarity.

Table 2. Selected bond lengths [Å] and angles [°] for compound **1a**.

P1–C3	1.857(2)	N3–C2	1.462(3)
P1–C1	1.857(2)	N3–C4	1.476(3)
P1–C4	1.857(3)	C3–P1–C1	96.98(11)
O1–C8	1.201(3)	C3–P1–C4	96.04(11)
N1–C7	1.494(3)	C1–P1–C4	95.63(12)
N1–C3	1.518(3)	C7–N1–C3	112.52(18)
N1–C6	1.544(3)	C7–N1–C6	112.00(18)
N1–C5	1.554(3)	C3–N1–C6	110.60(17)
N2–C5	1.424(3)	C7–N1–C5	104.95(16)
N2–C2	1.471(3)	C3–N1–C5	109.26(17)
N2–C1	1.469(3)	C6–N1–C5	107.20(17)
N3–C6	1.431(3)		

long phenyl-ring interactions [closest centroid...centroid distances of 4.934(2) Å, interplanar angle of 0° and perpendicular distances of 3.095 Å with slippage of 3.845 Å].

Table 3. Selected bond lengths [Å] and angles [°] for compound **1b**.

N1–C9	1.512(3)	C9–N1–C10	109.4(2)
N1–C7	1.515(3)	C7–N1–C10	111.4(2)
N1–C10	1.538(3)	C9–N1–C8	110.2(2)
N1–C8	1.542(3)	C7–N1–C8	106.6(2)
N2–C8	1.432(4)	C10–N1–C8	107.5(2)
N2–C13	1.461(4)	C8–N2–C13	109.5(2)
N2–C11	1.475(4)	C8–N2–C11	112.0(2)
N3–C10	1.440(4)	C13–N2–C11	111.9(2)
N3–C13	1.467(4)	C10–N3–C13	110.2(2)
N3–C12	1.474(4)	C10–N3–C12	112.7(2)
P1–C11	1.836(3)	C13–N3–C12	111.1(2)
P1–C9	1.841(3)	C11–P(1–C9	96.69(14)
P1–C12	1.841(3)	C11–P1–C12	95.75(14)
C9–N1–C7	111.6(2)	C9–P1–C12	96.25(13)

Table 4. Selected bond lengths [Å] and angles [°] for compound **3**.^[a]

Au1–P1	2.405(3)	C1–P1–C2	90.5(6)
Au1–Br1	2.5980(14)	C3–P1–C2	102.4(5)
Au1–Au1 ^{#1}	2.8439(11)	C1–P1–Au1	129.2(4)
P1–C1	1.780(11)	C1–P1–C3	96.2(5)
P1–C3	1.787(11)	C3–P1–Au1	111.7(4)
P1–C2	1.875(12)	C2–P1–Au1	121.5(4)
N1–C7	1.486(13)	C4–N3–C6	116.5(8)
N1–C4	1.465(13)	C4–N3–C1	108.0(9)
N1–C5	1.551(13)	C6–N3–C1	115.0(8)
N1–C3	1.603(14)	C6–N2–C5	106.8(9)
N2–C2	1.600(15)	C6–N2–C2	118.2(9)
N2–C6	1.407(14)	C5–N2–C2	107.4(9)
N2–C5	1.424(14)	C4–N1–C7	105.6(8)
N3–C4	1.403(13)	C4–N1–C5	101.2(8)
N3–C6	1.470(14)	C7–N1–C5	112.5(8)
N3–C1	1.563(14)	C4–N1–C3	116.4(8)
P1–Au1–Br1	174.37(7)	C7–N1–C3	107.2(8)
P1–Au1–Au1 ^{#1}	91.66(7)	C5–N1–C3	113.8(8)
Br1–Au1–Au1 ^{#1}	91.52(4)		

[a] ^{#1} $-x + 2, y, -z + 3/2$.

Complex **5b** crystallises in the space group $C2/c$ and contains an asymmetric unit that consists of two symmetry-related gold molecules with a crossed structure (torsion angle of 119°) and short Au...Au interactions of 2.8439(11) Å (Figure 4). Similar structures have been found in the PTA-gold(I) derivatives: [AuCl(PTA)], [AuCl(PTA-HCl)] and [AuBr(PTA)].^[41] in which the dimers are connected by longer Au...Au contacts of 3.092(1), 3.322(1) and 3.107(2) Å, respectively. The presence of short intermolecular gold-gold contacts is typical for gold(I) complexes. These interactions normally display values over 3 Å, except for ligands that exhibit additional hydrogen bonding,^[44–47] in which shorter distances are found. Complex **5b** is a special case as there is no hydrogen bonding between the PTA molecules. As such, relative to previously reported gold PTA derivatives, the most spatially demanding phosphane [PTA-CH₂Ph]Br gives the shortest metallic interactions. This is due to the fact that the dimers associate (Figure 5) by means of N3...C4 intermolecular contacts of 3.037(17) Å between the PTA molecules [C4-H4b...N3ⁱ 2.49 Å, C4...N3ⁱ 3.037(17) Å and angle at H4b of 115° for $i: 1/2 - x, 1/2 - y,$

$1 - z$]. The geometry around the N atoms in the PTA molecule is similar to that in the free phosphane **1b**, with a distorted-pyramidal geometry around N2 and N3 [average C–N–C angles of 110.8(9) and 113.16°] and an almost ideal tetrahedral geometry for the quaternary N1 atom [average C–N–C angles of 109.45(8)°]. Although the N–C bond lengths for the quaternary nitrogen N1 are longer than those observed for N2 and N3, as is also the case for **1b**, this difference is less pronounced than in free PTA [N1–C 1.5262(13) Å, N2–C 1.477(14) Å, N3–C 1.4786(14) Å on average]. As expected, the coordination geometry at the Au centre is essentially linear with a P1–Au1–Br1 bond angle of 174.37(7)°. The Au–P bond length of 2.5980(14) Å compares well with previously reported gold-PTA derivatives.^[28,29,31,41,48–51] However, the Au–Br bond length of 2.5980(14) Å is 0.22 Å longer than that described in [AuBr(PTA)].^[41]

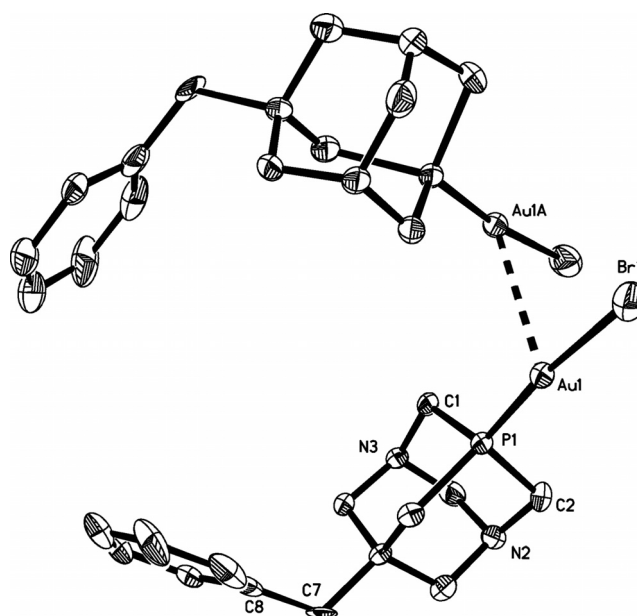


Figure 4. Molecular structure of [AuBr(PTA-CH₂Ph)]Br (**5b**) showing the cation. Thermal ellipsoids are drawn at the 50% probability level. Hydrogen atoms are omitted for clarity.

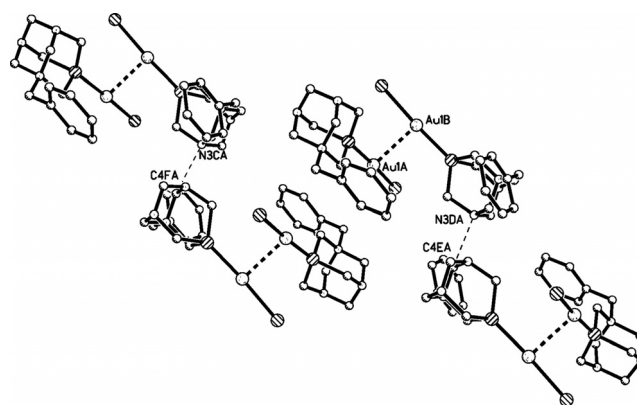


Figure 5. View of the packing in the unit cell of complex **5b**.

Cytotoxic Assays

We have evaluated the cytotoxic properties of some of these phosphane derivatives (Table 5) against the cisplatin-sensitive human ovarian carcinoma A2780 cell lines and its cisplatin-resistant counterpart A2780cisR. For comparison purposes, the cytotoxicity of cisplatin was also evaluated under the same experimental conditions. To avoid any possible interchange between the anion coordinated to gold and the counterion, we only studied samples with the same anion and counterion, namely, $[\text{AuX}(\text{PTA}-\text{CH}_2\text{CO}_2\text{Me})]\text{X}$ [$\text{X} = \text{Cl}$ (**4a**), Br (**4b**)] and $[\text{AuX}(\text{PTA}-\text{CH}_2\text{Ph})]\text{X}$ [$\text{X} = \text{Cl}$ (**5a**), Br (**5b**)]. The four complexes display very high cytotoxicities, with IC_{50} values that range from 0.05 to 0.08 μM for the sensitive A2780 cell lines, thus making them much more potent than cisplatin. In the best case (**5a**), the IC_{50} value is almost 18-fold lower than that found for cisplatin. Higher IC_{50} values (in the range 0.3 to 0.6 μM) are observed in all cases for the resistant A2780 cell lines, although they remain lower than that found for cisplatin (11-fold lower in the best cases of **4a** and **4b**). The four complexes exhibit greater cytotoxicities in both cell lines than previously reported gold(I) derivatives that contain PTA and thiolate or alkylne ligands.^[28,29]

Table 5. IC_{50} values in A2780 cell lines and distribution coefficients of $[\text{AuX}(\text{PTA}-\text{R})]\text{X}$ complexes and cisplatin.

	IC_{50} [μM] ^[a]		$\log D_{7.4}$
	A2780	A2780cisR	
$[\text{AuCl}(\text{PTA}-\text{CH}_2\text{CO}_2\text{Me})]\text{Cl}$ (4a)	0.088 ± 0.001	0.318 ± 0.012	−0.40
$[\text{AuBr}(\text{PTA}-\text{CH}_2\text{CO}_2\text{Me})]\text{Br}$ (4b)	0.082 ± 0.001	0.318 ± 0.018	−0.34
$[\text{AuCl}(\text{PTA}-\text{CH}_2\text{Ph})]\text{Cl}$ (5a)	0.050 ± 0.001	0.408 ± 0.012	−0.39
$[\text{AuBr}(\text{PTA}-\text{CH}_2\text{Ph})]\text{Br}$ (5b)	0.057 ± 0.001	0.617 ± 0.021	−0.14
cisplatin	0.943 ± 0.013	3.676 ± 0.21	

[a] Mean \pm SE of at least three determinations.

Berners-Price et al.^[52] have previously shown that an optimal balance between the lipophilic and hydrophilic nature of metal-based drugs is one of the most important factors for antitumor activity. In our case, the lipophilicity/hydrophilicity covers a narrow range, with distribution coefficients ($\log D_{7.4}$) of between −0.14 and −0.40 (Table 5), thus indicating a balanced relationship between their lipophilic and hydrophilic character. It has been found that gold derivatives with a high lipophilic character, such as $[\text{Au}(\text{dppe})_2]\text{Cl}$ [$\log P = +1.41$; dppe = 1,2-bis(diphenylphosphino)ethane] lead to high host toxicity as a consequence of nonspecific binding to biomolecules, whereas other, more hydrophilic gold complexes might be more easily excreted as a result of low protein binding.^[52]

Conclusion

Phosphanes derived from PTA can easily be synthesised by alkylation of one of the N atoms of the PTA molecule upon treatment of PTA with the appropriate alkyl bromide salts. Coordination of these phosphanes to gold(I) deriv-

atives gives water-soluble compounds of the type $[\text{AuX}(\text{PTA}-\text{R})]\text{Br}$ ($\text{X} = \text{Cl}$, C_6F_5), in which a fast interchange between the bromide counterion and the anion coordinated to the metallic centre is observed in solution, thus giving rise to a mixture of complexes.

The substitution of chlorine by bromine in the chlorido-gold derivative, or use of the corresponding chlorine-containing PTA, namely, $[(\text{PTA}-\text{R})]\text{Cl}$, as starting material leads to the preparation of pure $[\text{AuX}(\text{PTA}-\text{R})]\text{X}$ ($\text{X} = \text{Cl}$, Br ; $\text{R} = -\text{CH}_2\text{Ph}$, $-\text{CH}_2\text{CO}_2\text{Me}$) derivatives. These pure compounds were tested for their antiproliferative activity against the human ovarian cancer cell lines A2780/S and A2780/R. In all cases they showed a better cytotoxicity than cisplatin. A balanced relationship between lipophilicity and hydrophilicity is found in these derivatives, which is one of the requisites during the synthesis of an anticancer drug to facilitate its administration and transport in the body and avoid host toxicity.

Experimental Section

General: ^1H , $^{31}\text{P}\{^1\text{H}\}$ (161.97 MHz), $^{13}\text{C}\{^1\text{H}\}$ (100.62 or 75.4 MHz) and $^{19}\text{F}\{^1\text{H}\}$ (376 MHz) NMR spectra were recorded with 400 or 300 MHz Bruker Avance spectrometers. Chemical shifts are quoted relative to external TMS (^1H , ^{13}C) or 85% H_3PO_4 (^{31}P) or to CFCl_3 (^{19}F); coupling constants are reported in Hz. MALDI mass spectra were measured with a Micromass Autospec spectrometer in positive-ion mode using *trans*-2-[3-(4-*tert*-butylphenyl)-2-methyl-2-propenylidene]malonitrile (DCTB) as matrix. IR spectra were recorded with a Perkin–Elmer Spectrum 100 FTIR (far-IR) spectrometer. Steady-state photoluminescence spectra were recorded with a Jobin–Yvon–Horiba fluorolog FL-3-11 spectrometer using band pathways of 3 nm for both excitation and emission. Elemental analyses were obtained in-house with a LECO CHNS-932 microanalyser. The phosphane PTA^[9] and the related molecules $[\text{PTA}-\text{R}]\text{X}$ [$\text{R} = -\text{CH}_2\text{COOMe}$ (**1a**), $-\text{CH}_2\text{Ph}$ (**1b**), $-\text{CH}_2\text{CN}$ (**1c**); $\text{X} = \text{Br}$]^[17] ($\text{R} = -\text{CH}_2\text{Ph}$, $\text{X} = \text{Cl}$)^[14,15,53,54] were prepared according to published methods. The compounds of $[\text{AuCl}(\text{PTA}-\text{R})]\text{Br}$ [$\text{R} = -\text{CH}_2\text{COOMe}$ (**3a**), $-\text{CH}_2\text{Ph}$ (**3b**)] were prepared as published elsewhere.^[17]

Preparation of $[\text{PTA}-\text{R}]\text{Br}$ [$\text{R} = -\text{CH}_2\text{C}\equiv\text{CH}$ (1d**), $-\text{CH}_2\text{CONH}_2$ (**1e**), $-\text{CH}_2\text{COOH}$ (**1f**):** A solution of RBr (2 mmol) in acetone (ca. 10 mL) was added dropwise to a solution of PTA (2 mmol, 0.314 g) in acetone (ca. 10 mL) at room temperature. After stirring the mixture for approximately 25 min, the white solids were isolated by filtration, washed with acetone and diethyl ether and dried in air.

$[\text{PTA}-\text{CH}_2\text{C}\equiv\text{CH}]\text{Br}$ (1d**):** Yield 83%, white solid. ^1H NMR ($[\text{D}_6]-\text{DMSO}$, 25 °C): $\delta = 5.02$ and 4.94 (AB system, $J_{\text{A,B}} = 11.2$ Hz, 4 H, NCH_2N), 4.55 (d, $J_{\text{H,H}} = 13.4$ Hz, 1 H, NCH_2N), 4.44 (d, $J_{\text{H,H}} = 6.2$ Hz, 2 H, NCH_2P), 4.33 (d, $J_{\text{H,H}} = 13.4$ Hz, 1 H, NCH_2N), 4.08 (t, $J_{\text{H,H}} = 2.6$ Hz, 1 H, $\text{CH}_2\text{C}\equiv\text{CH}$), 3.96 (d, $J_{\text{H,H}} = 2.6$ Hz, 2 H, $\text{CH}_2\text{C}\equiv\text{CH}$), 3.93–3.86 (m, 4 H, NCH_2P) ppm. $^{31}\text{P}\{^1\text{H}\}$ NMR ($[\text{D}_6]\text{DMSO}$): $\delta = -81.7$ ppm. $^{13}\text{C}\{^1\text{H}\}$ NMR (100.62 MHz, $[\text{D}_6]\text{DMSO}$): $\delta = 84.2$ (s, $\text{C}\equiv\text{CH}$), 79.3 (s, 2 C, NCH_2N), 70.9 (s, $\text{C}\equiv\text{CH}$), 69.7 (s, NCH_2N), 53.6 (d, $J_{\text{PC}} = 45.2$ Hz, PCH_2N), 51.3 (s, $\text{CH}_2\text{C}\equiv\text{CH}$), 45.7 (d, $J_{\text{PC}} = 27.1$ Hz, PCH_2N) ppm. MALDI MS: m/z (%) = 196.1 (100) $[\text{M}]^+$. IR: $\tilde{\nu} = 2114$ cm^{-1} [$\nu(\text{C}\equiv\text{C})$]. $\text{C}_9\text{H}_{15}\text{BrN}_3\text{P}$ (276.11): calcd. C 39.15, H 5.47, N 15.22; found C 38.66, H 5.59, N 15.16. $\text{S}_{25^\circ\text{C}}(\text{H}_2\text{O})$: 13 g L^{-1} .

**[PTA-CH₂CONH₂]
Br (1e):** Yield 84%, white solid. ¹H NMR ([D₆]DMSO, 25 °C): δ = 8.01 (s, 1 H, NH₂), 7.73 (s, 1 H, NH₂), 5.28 and 5.06 (AB system, J_{A,B} = 10.8 Hz, 4 H, NCH₂N), 4.62 (s, 2 H, NCH₂P), 4.55 (d, J_{H,H} = 14 Hz, 1 H, NCH₂N), 4.36 (d, J_{H,H} = 13.6 Hz, 1 H, NCH₂N), 3.98–3.84 (m, 4 H, NCH₂P), 3.66 (s, 2 H, CH₂CO) ppm. ³¹P{¹H} NMR ([D₆]DMSO): δ = –84.4 ppm. ¹³C{¹H} NMR (100.62 MHz, [D₆]DMSO): δ = 165.15 (s, CO), 80.20 (s, 2 C, NCH₂N), 69.82 (s, NCH₂N), 60.62 (s, CH₂CO), 53.4 (d, J_{P,C} = 32.7 Hz, PCH₂N), 46.1 (d, J_{P,C} = 20.2 Hz, PCH₂N) ppm. MALDI MS: *m/z* (%) = 215.3 (61) [M]⁺. IR: ν̄ = 1696 cm^{–1} [ν(C=O)]. C₈H₁₆BrN₄OP (295.12): calcd. C 32.56, H 5.46, N 18.98; found C 32.64, H 5.89, N 19.38. S_{25°C}(H₂O): 733 g L^{–1}.

**[PTA-CH₂COOH]
Br (1f):** Yield 78%, white solid. ¹H NMR ([D₆]DMSO, 25 °C): δ = 5.09 (AB system, J_{A,B} = 11.3 Hz, 4 H, NCH₂N), 4.7 (d, J_{H,H} = 10.9 Hz, 1 H, NCH₂N), 4.6 (d, J_{H,H} = 8 Hz, 2 H, NCH₂P), 4.33 (d, J_{H,H} = 13.4 Hz, 1 H, NCH₂N), 3.88–3.78 (m, 4 H, NCH₂P), 3.5 (s, 1 H, CH₂OOH) ppm. ³¹P{¹H} NMR ([D₆]DMSO): δ = –85.28 ppm. ¹³C{¹H} NMR (100.62 MHz, [D₆]DMSO): δ = 165.2 (s, CO), 79.5 (s, NCH₂N), 71.2 (s, NCH₂N), 61.7 (s, CH₂COOH), 52.9 (d, J_{P,C} = 31.2 Hz, PCH₂N), 46.2 (d, J_{P,C} = 20.1 Hz, PCH₂N) ppm. MALDI MS (%) *m/z* (%) = 216 (14.21) [M]⁺. IR: ν̄ = 1684 cm^{–1} [ν(C=O)]. C₈H₁₆BrN₄OP (296.1): calcd. C 32.45, H 5.11, N 14.19; found C 32.72, H 5.4, N 14.47. S_{25°C}(H₂O): 582 g L^{–1}.

Preparation of [PTA-R]Cl [R = –CH₂CO₂Me (2a)]: A solution of RCl in acetone (2 mmol) was added to a solution of PTA (2 mmol, 0.314 g) in acetone (ca. 10 mL) heated at reflux. After stirring the mixture for approximately 24 h, the white solids were isolated by filtration, washed with acetone and diethyl ether and dried in air. Yield 80%, white solid. ¹H NMR ([D₆]DMSO, 25 °C): δ = 5.26 and 5.13 (AB system, J_{A,B} = 11.2 Hz, 4 H, NCH₂N), 4.63 (d, J_{H,H} = 5.6 Hz, 2 H, NCH₂P), 4.57–4.41 (m, 2 H, NCH₂N), 4.04 (s, 2 H, CH₂COOMe), 3.98–3.87 (m, 4 H, NCH₂P), 3.77 (s, 3 H, Me) ppm. ³¹P{¹H} NMR ([D₆]DMSO): δ = –84.4 ppm. ¹³C{¹H} NMR (75.4 MHz, [D₆]DMSO): δ = 165 (s, CO), 79.8 (s, NCH₂N), 70.2 (s, NCH₂N), 59.9 (s, CH₂CO), 53.8 (d, PCH₂N), 53.5 (s, Me), 45.9 (d, PCH₂N) ppm. MALDI MS: *m/z* (%) = 229.8 (100) [M]⁺. IR: ν̄ = 1745 cm^{–1} [ν(C=O)]. C₉H₁₇ClN₃O₂P (265.68): calcd. C 40.69, H 6.45, N 15.82; found C 40.18, H 6.99, N 15.47. S_{25°C}(H₂O): 2586 g L^{–1}.

Preparation of [AuCl(PTA-R)]Br Complexes [R = –CH₂CN (3c), –CH₂C≡CH (3d), –CH₂CONH₂ (3e), –CH₂COOH (3f)]: [PTA-R]Br (0.2 mmol) was added to a solution of [AuCl(tht)] (0.2 mmol; 0.0641 g) in acetone (ca. 10 mL). After stirring the mixture for approximately 4 h, the solutions were concentrated and the addition of Et₂O precipitated the products, which were isolated by filtration and dried in air as white solids.

[AuCl(PTA-CH₂CN)]Br (3c): Yield 76%, white solid. ¹H NMR ([D₆]DMSO, 25 °C): δ = 5.28 and 5.19 (AB system, J_{H,H} = 12 Hz, 4 H, NCH₂N), 4.73 (s, 2 H, NCH₂P), 4.65 (d, J_{H,H} = 13.4 Hz, 1 H, NCH₂N), 4.58 (s, 2 H, CH₂CN), 4.38–4.46 (m, 1 H, NCH₂N), 4.01–4.13 (m, 4 H, NCH₂P) ppm. ³¹P{¹H} NMR ([D₆]DMSO): δ = –75.5 ppm. ¹³C{¹H} NMR (100.62 MHz, [D₆]DMSO): δ = 111.3 (s, CN), 80.6 (s, NCH₂N), 69.2 (s, NCH₂N), 55.1 (d, J_{P,C} = 26.1 Hz, PCH₂N), 48.3 (s, CH₂CN), 46.5 (d, J_{P,C} = 14 Hz, PCH₂N) ppm. IR: ν̄ = 1682 cm^{–1} [ν(C≡N)]. C₈H₁₄AuBrClN₄P (509.52): calcd. C 18.86, H 2.77, N 11.00; found C 19.35, H 2.73, N 11.38. S_{25°C}(H₂O): 65.21 g L^{–1}.

[AuCl(PTA-CH₂C≡CH)]Br (3d): Yield 85%, white solid. ¹H NMR ([D₆]DMSO, 25 °C): δ = 5.03 and 5.12 (AB system, J_{H,H} = 11.2 Hz, 4 H, NCH₂N), 4.89 (d, J_{H,H} = 5.3 Hz, 2 H, NCH₂P), 4.66 (d, J_{H,H} = 13.4 Hz, 1 H, NCH₂N), 4.28–4.43 (m, 5 H, NCH₂N + NCH₂P),

4.17 (br. s, 1 H, CH₂C≡CH), 4.11 (br. s, 2 H, CH₂C≡CH) ppm. ³¹P{¹H} NMR ([D₆]DMSO): δ = –29.7 ppm. ¹³C{¹H} NMR (75.4 MHz, [D₆]DMSO): δ = 84.9 (s, C≡CH), 78.5 (s, NCH₂N), 70.3 (s, NCH₂N), 55.9 (d, J_{P,C} = 23.4 Hz, PCH₂N), 51.3 (s, CH₂C≡CH), 47.9 (d, J_{P,C} = 22 Hz, PCH₂N) ppm. MALDI MS: *m/z* (%) = 507 (18) [M + Br]⁺. IR: ν̄ = 2118 cm^{–1} [ν(C≡C)]. C₉H₁₅AuBrClN₃P (508.53): calcd. C 21.26, H 2.97, N 8.26; found C 21.8, H 2.51, N 8.66. S_{25°C}(H₂O): 7.4 g L^{–1}.

[AuCl(PTA-CH₂CONH₂)]Br (3e): Yield 76%, white solid. ¹H NMR ([D₆]DMSO, 25 °C): δ = 8.09 (s, 1 H, NH₂), 7.83 (s, 1 H, NH₂), 5.38 and 5.12 (AB system, J_{A,B} = 11.2 Hz, 4 H, NCH₂N), 4.99 (d, J_{H,H} = 4 Hz, 2 H, NCH₂P), 4.62–4.58 (m, 1 H, NCH₂N), 4.4–4.32 (m, 4 H, NCH₂N and NCH₂P), 3.79 (s, 2 H, CH₂CO) ppm. ³¹P{¹H} NMR ([D₆]DMSO): δ = –34.1 ppm. ¹³C{¹H} NMR (75.4 MHz, [D₆]DMSO): δ = 165.1 (s, CO), 80.1 (s, NCH₂N), 69.7 (s, NCH₂N), 60.5 (s, CH₂CO), 53.7 (d, J_{P,C} = 28 Hz, PCH₂N), 46.5 (d, J_{P,C} = 16.6 Hz, PCH₂N) ppm. MALDI MS: *m/z* (%) = 449 (22) [M]⁺. C₈H₁₆AuBrClN₄OP (527.74): calcd. C 18.21, H 3.06, N 10.62; found C 18.83, H 3.12, N 10.41. S_{25°C}(H₂O): 243 g L^{–1}.

[AuCl(PTA-CH₂COOH)]Br (3f): Yield 78%, white solid. ¹H NMR ([D₆]DMSO, 25 °C): δ = 5.09–5.29 (AB system, J_{A,B} = 11.3 Hz, 4 H, NCH₂N), 4.78 (d, J_{H,H} = 4 Hz, 2 H, NCH₂P), 4.65 (d, J_{H,H} = 10.7 Hz, 1 H, NCH₂N), 4.31 (d, J_{H,H} = 13.4 Hz, 1 H, NCH₂N), 3.95 (d, J_{H,H} = 8.7 Hz, 2 H, CH₂CO), 3.75 (m, 4 H, NCH₂P), 3.65 (s, 1 H, COOH) ppm. ³¹P{¹H} NMR ([D₆]DMSO): δ = –31.7 ppm. ¹³C{¹H} NMR (75.4 MHz, [D₆]DMSO): δ = 165.4 (s, CO), 79.6 (s, NCH₂N), 71.7 (s, NCH₂N), 61.0 (s, CH₂COOH), 53.7 (d, J_{P,C} = 41 Hz, PCH₂N), 46.5 (d, J_{P,C} = 19 Hz, PCH₂N) ppm. MALDI MS: *m/z* (%) = 216 (14) [M]⁺, 447 (2) [M – H]⁺. IR: ν̄ = 1684 cm^{–1} [ν(C=O)]. C₈H₁₅AuBrClN₃O₂P (528.52): calcd. C 18.18, H 2.86, N 7.95; found C 18.3, H 2.7, N 7.14. S_{25°C}(H₂O): 180 g L^{–1}.

Preparation of [AuCl(PTA-R)]Cl Complexes [R = –CH₂CO₂Me (4a), –CH₂Ph (4b)]: [PTA-R]Cl (0.2 mmol) was added to a solution of [AuCl(tht)] (0.2 mmol; 0.0641 g) in acetone (ca. 10 mL). After stirring the mixture for approximately 4 h, the solutions were concentrated and the addition of Et₂O precipitated the products, which were isolated by filtration, dried in air as white solids and recrystallised from MeOH/OEt₂.

[AuCl(PTA-CH₂CO₂Me)]Cl (4a): Yield 86%, white solid. ¹H NMR ([D₆]DMSO, 25 °C): δ = 5.27 and 5.39 (AB system, J_{A,B} = 11.2 Hz, 4 H, NCH₂N), 5.06 (d, J_{H,H} = 5.6 Hz, 2 H, PCH₂N), 4.59–4.52 (m, 2 H, NCH₂N), 4.36–4.47 (m, 4 H, PCH₂N + CH₂COOMe), 4.2 (s, 2 H, CH₂Ph), 3.79 (s, 3 H) ppm. ³¹P{¹H} NMR ([D₆]DMSO): δ = –31.7 ppm. ¹³C{¹H} NMR (100.62 MHz, [D₆]DMSO): δ = 164.5 (s, CO), 80.75 (s, NCH₂N), 69.08 (s, NCH₂N), 59.7 (s, CH₂COOMe), 54.05 (d, J_{P,C} = 27.6 Hz, PCH₂N), 53.57 (s, COOMe), 48.22 (d, J_{P,C} = 20.8 Hz, PCH₂N) ppm. MALDI MS: *m/z* (%) = 462 (11) [M]⁺. IR: ν̄ = 1746 cm^{–1} [ν(CO)]. C₉H₁₇AuCl₂N₃O₂P (498.1): calcd. C 21.70, H 3.44, N 8.44; found C 22.02, H 3.8, N 8.13. S_{25°C}(H₂O): 30 g L^{–1}.

[AuCl(PTA-CH₂Ph)]Cl (4b): Yield 97%, white solid. ¹H NMR ([D₆]DMSO, 25 °C): δ = 7.55–7.61 (m, 5 H, Ph), 4.97 and 5.22 (AB system, J_{A,B} = 11.6 Hz, 4 H, NCH₂N), 4.65 (d, J_{H,H} = 5.6 Hz, 2 H, NCH₂P), 4.57 (d, J_{H,H} = 13.1 Hz, 1 H, NCH₂N), 4.38–4.22 (m, 7 H, NCH₂P + NCH₂N + CH₂Ph) ppm. ³¹P{¹H} NMR ([D₆]DMSO): δ = –30.4 ppm. ¹³C{¹H} NMR (100.62 MHz, [D₆]DMSO): δ = 135.5, 130.9, 129.6 (s, Ph), 78.9 (s, NCH₂N), 69.1 (s, NCH₂N), 64.7 (s, CH₂Ph), 52.3 (d, J_{P,C} = 23 Hz, PCH₂N), 47.9 (d, J_{P,C} = 23 Hz, PCH₂N) ppm. MALDI MS: *m/z* (%) = 480.2 (100) [M]⁺. C₁₃H₁₉AuCl₂N₃P (516.16): calcd. C 30.25, H 3.71, N 8.14; found C 30.04, H 3.75, N 8.19.

Preparation of [AuBr(PTA-R)]Br Complexes [R = -CH₂CO₂Me (5a), -CH₂Ph (5b)]: NaBr was added in an excess amount to a solution of [AuCl(PTA-R)]Br (0.2 mmol) in acetone (ca. 10 mL). After stirring the mixture for approximately 24 h, the solutions were concentrated and the addition of Et₂O precipitated the products, which were isolated by filtration, dried in air as white solids and recrystallised from MeOH/OEt₂.

[AuBr(PTA-CH₂CO₂Me)]Br (5a): Yield 96%, white solid. ¹H NMR ([D₆]DMSO, 25 °C): δ = 5.20 and 5.36 (AB system, J_{A,B} = 11.2 Hz, 4 H, NCH₂N), 4.96 (br. s, 2 H, PCH₂N), 4.58 (d, J_{H,H} = 13.2 Hz, 1 H, NCH₂N), 4.27–4.38 (m, 5 H, PCH₂N + NCH₂N), 4.12 (s, 2 H, CH₂COOMe), 3.78 (s, 3 H) ppm. ³¹P{¹H} NMR ([D₆]DMSO): δ = -41.6 ppm. ¹³C{¹H} NMR (75.4 MHz, [D₆]DMSO): δ = 164.4 (s, CO), 80.6 (s, NCH₂N), 68.9 (s, NCH₂N), 59.6 (s, CH₂CO), 54.2 (d, J_{P,C} = 18.1 Hz, PCH₂N), 53.6 (s, Me), 48.2 (d, J_{P,C} = 19.6 Hz, PCH₂N) ppm. MALDI MS: m/z (%) = 508 (100) [M]⁺. IR: ν̄ = 1752 cm⁻¹ [ν(CO)]. C₉H₁₇AuBr₂N₃O₂P (584.91): calcd. C 18.42, H 2.92, N 7.16; found C 18.09, H 2.61, N 6.84. S_{25°C}(H₂O): 20 g L⁻¹.

[AuBr(PTA-CH₂Ph)]Br (5b): Yield 78%, white solid. ¹H NMR ([D₆]DMSO, 25 °C): δ = 7.53–7.60 (m, 5 H, Ph), 4.35 and 5.03 (AB system, J_{A,B} = 8 Hz, 4 H, NCH₂N), 4.75 (d, J = 8 Hz, 2 H, NCH₂P), 4.58–4.62 (m, 1 H, NCH₂N), 4.37–4.44 (m, 3 H, NCH₂N + NCH₂P), 4.37 (s, 2 H, CH₂Ph), 4.26–4.30 (m, 2 H, NCH₂P) ppm. ³¹P{¹H} NMR ([D₆]DMSO): δ = -39.1 ppm. ¹³C{¹H} NMR (100.62 MHz, [D₆]DMSO): δ = 133.7, 129.3 (s, Ph), 78.5 (s, NCH₂N), 69.1 (s, NCH₂N), 64.1 (s, CH₂Ph), 52.1 (d, J_{P,C} = 30 Hz, PCH₂N), 47.6 (d, J_{P,C} = 20.1 Hz, PCH₂N) ppm. C₁₃H₁₉AuBr₂N₃P (602.93): calcd. C 25.81, H 3.17, N 6.94; found C 25.78, H 2.68, N 6.54.

Preparation of [Au(C₆F₅)(PTA-R)]Br Complexes [R = -CH₂CO₂Me (6a), -CH₂Ph (6b), -CH₂CN (6c), -CH₂C≡CH (6d), -CH₂CONH₂ (6e)]: [PTA-R]Br (0.2 mmol) was added to a solution of [Au(C₆F₅)(tht)] (0.2 mmol; 0.0904 g) in acetone (ca. 10 mL). After stirring the mixture for approximately 4 h, the solutions were concentrated and the addition of Et₂O precipitated the products, which were isolated by filtration, dried in air as white solids and recrystallised from MeOH/OEt₂.

[Au(C₆F₅)(PTA-CH₂CO₂Me)]Br (6a): Yield 81%, white solid. ¹H NMR ([D₆]DMSO, 25 °C): δ = 3.79 (s, 3 H, COOMe), 4.08 (s, 2 H, CH₂COOMe), 4.22–4.39 (m, 5 H, NCH₂N + NCH₂P), 4.62 (d, J_{H,H} = 13.2 Hz, 1 H, NCH₂N), 4.91 (s, 2 H, NCH₂P), 5.13 and 5.35 (AB system, J_{A,B} = 11.2 Hz, 4 H, NCH₂N) ppm. ³¹P{¹H} NMR ([D₆]DMSO): δ = -31.1 ppm. ¹⁹F{¹H} NMR ([D₆]DMSO): δ = -114.8 (m, F_{ortho}), -161.5 (t, F_{para}), -162.7 (m, F_{meta}) ppm. MALDI MS: m/z (%) = 594 (100) [M]⁺. IR: ν̄ = 1748 cm⁻¹ [ν(CO)]. C₁₅H₁₇AuBrF₅N₃O₂P (674.15): calcd. C 26.72, H 2.54, N 6.23; found C 26.45, H 2.94, N 6.02. S_{25°C}(H₂O): 42 g L⁻¹.

[Au(C₆F₅)(PTA-CH₂Ph)]Br (6b): Yield 84%, white solid. ¹H NMR ([D₆]DMSO, 25 °C): δ = 7.55–7.6 (m, 5 H, Ph), 4.97 and 5.18 (AB system, J_{A,B} = 11.6 Hz, 4 H, NCH₂N), 4.56–4.63 (m, 3 H, NCH₂N + NCH₂P), 4.26 (s, 2 H, CH₂Ph), 4.20–4.45 (m, 5 H, NCH₂P) ppm. ³¹P{¹H} NMR ([D₆]DMSO): δ = -29.9 ppm. ¹⁹F{¹H} NMR ([D₆]DMSO): δ = -114.5 (m, F_{ortho}), -161.4 (t, F_{para}), -162.7 (m, F_{meta}) ppm. ¹³C{¹H} NMR (75.4 MHz, [D₆]DMSO): δ = 133.4, 130.6, 129.4 (s, Ph), 126.3 (s, C₆F₅), 78.9 (s, NCH₂N), 69.6 (s, NCH₂N), 64.9 (s, CH₂Ph), 52.4 (d, J_{P,C} = 28.6 Hz, PCH₂N), 46.4 (d, J_{P,C} = 18.9 Hz, PCH₂N) ppm. MALDI MS: m/z (%) = 612 (100) [M]⁺, 524 (40) [M - C₆F₅ + Br]⁺. C₁₉H₁₉AuBrF₅N₃P (692.21): calcd. C 32.97, H 2.77, N 6.07; found C 32.59, H 3.73, N 6.42. S_{25°C}(H₂O): 3.6 g L⁻¹.

[Au(C₆F₅)(PTA-CH₂C≡CH)]Br (6d): Yield 84%, white solid. ¹H NMR ([D₆]DMSO, 25 °C): δ = 4.99 and 5.11 (AB system, J_{A,B} = 11.2 Hz, 4 H, NCH₂N), 4.83 (br. s, 2 H, NCH₂P), 4.57 (d, J_{H,H} = 13.6 Hz, 1 H, NCH₂N), 4.27–4.44 (m, 5 H, NCH₂N + NCH₂P), 4.19 (br. s, 1 H, CH₂C≡CH), 4.09 (br. s, 2 H, CH₂C≡CH) ppm. ³¹P{¹H} NMR ([D₆]DMSO): δ = -28.5 ppm. ¹⁹F{¹H} NMR ([D₆]DMSO): δ = -114.3 (m, F_{ortho}), -161.7 (t, F_{para}), -163.1 (m, F_{meta}) ppm. ¹³C{¹H} NMR (75.4 MHz, [D₆]DMSO): δ = 126.5 (s, C₆F₅), 84.3 (s, C≡CH), 79.3 (s, NCH₂N), 69.7 (s, NCH₂N), 69.4 (s, C≡CH), 53.4 (d, J_{P,C} = 15 Hz, PCH₂N), 49.5 (s, CH₂C≡CH), 46.0 (d, J_{P,C} = 18.8 Hz, PCH₂N) ppm. MALDI MS: m/z (%) = 521 (22) [M - CH₂CCH]⁺. IR: ν̄ = 2166 cm⁻¹ [ν(C≡C)]. C₁₅H₁₅AuBrF₅N₃P (640.14): calcd. C 28.14, H 2.36, N 6.56; found C 28.05, H 2.78, N 6.83. S_{25°C}(H₂O): 5.5 g L⁻¹.

[Au(C₆F₅)(PTA-CH₂CONH₂)]Br (6e): Yield 76%, white solid. ¹H NMR ([D₆]DMSO, 25 °C): δ = 8.02 (s, 1 H, NH₂), 7.80 (s, 1 H, NH₂), 5.33 and 5.05 (AB system, J_{A,B} = 11.2 Hz, 4 H, NCH₂N), 4.83 (s, 2 H, NCH₂P), 4.56–4.34 (m, 2 H, NCH₂N), 4.22–4.14 (m, 4 H, NCH₂P), 3.70 (s, 2 H, CH₂CO) ppm. ³¹P{¹H} NMR ([D₆]DMSO): δ = -53.7 ppm. ¹⁹F{¹H} NMR ([D₆]DMSO): δ = -114.5 (m, F_{ortho}), -161.3 (t, F_{para}), -162.5 (m, F_{meta}) ppm. MALDI MS: m/z (%) = 449 (22) [M]⁺. IR: ν̄ = 1685 cm⁻¹ [ν(C=O)]. C₁₄H₁₆AuBrF₅N₄OP (659.14): calcd. C 26.03, H 2.12, N 8.41; found C 25.51, H 2.45, N 8.50. S_{25°C}(H₂O): 40 g L⁻¹.

Preparation of [AuCl(PTA-R)₂](Br)₂ Complexes [R = -CH₂CO₂Me (7a), -CH₂Ph (7b), -CH₂C≡CH (7d)]: [PTA-R]Br (0.2 mmol) was added to a solution of [AuCl(PTA-R)]Br (0.2 mmol) in acetone (ca. 10 mL) at 0 °C. After stirring the mixture for approximately 4 h, the solutions were concentrated and the addition of Et₂O precipitated the products, which were isolated by filtration, dried in air as white solids and recrystallised from MeOH/OEt₂.

[AuCl(PTA-CH₂CO₂Me)₂](Br)₂ (7a): Yield 70%, white solid. ¹H NMR ([D₆]DMSO, 25 °C): δ = 5.16 and 5.33 (AB system, J_{A,B} = 11.2 Hz, 4 H, NCH₂N), 4.97 (d, J_{H,H} = 4.4 Hz, 2 H, PCH₂N), 4.57 (d, J_{H,H} = 13.2 Hz, 2 H, NCH₂N), 4.34–4.42 (m, 5 H, PCH₂N + NCH₂N), 4.1 (s, 2 H, CH₂COOMe), 3.79 (s, Me) ppm. ³¹P{¹H} NMR ([D₆]DMSO): δ = -34.3 ppm. MALDI MS: m/z (%) = 462 (6) [M - PTACH₂COOMe]⁺. IR: ν̄ = 1743 cm⁻¹ [ν(C=O)]. C₁₈H₃₄AuBr₂ClN₆O₄P₂ (852.68): calcd. C 25.35, H 4.02, N 9.86; found C 25.01, H 3.9, N 9.61. S_{25°C}(H₂O): 32.8 g L⁻¹.

[AuCl(PTA-CH₂Ph)₂](Br)₂ (7b): Yield 73%, white solid. ¹H NMR ([D₆]DMSO, 25 °C): δ = 7.54 (m, 5 H, Ph), 4.56 (d, J_{H,H} = 13.2 Hz, 1 H, NCH₂N), 4.91 and 5.11 (AB system, J_{A,B} = 11.2 Hz, 4 H, NCH₂N), 4.33 (d, J_{H,H} = 13.2 Hz, 1 H, NCH₂N), 4.12 (s, 2 H, NCH₂P), 4.18 (s, 2 H, CH₂Ph), 3.96–4.12 (m, 4 H, NCH₂P) ppm. ³¹P{¹H} NMR ([D₆]DMSO): δ = -59.9 ppm. C₂₆H₃₈AuBr₂ClN₆P (888.8): calcd. C 35.14, H 4.31, N 9.46; found C 35.42, H 4.62, N 9.81. S_{25°C}(H₂O): 7.5 g L⁻¹.

[AuCl(PTA-CH₂C≡CH)₂](Br)₂ (7d): Yield 70%, white solid. ¹H NMR ([D₆]DMSO, 25 °C): δ = 5.03 and 5.21 (AB system, J_{A,B} = 11.2 Hz, 4 H, NCH₂N), 4.77 (br. s, 2 H, NCH₂P), 4.63 (d, J_{H,H} = 13.2 Hz, 1 H, NCH₂N), 4.25–4.34 (m, 3 H, NCH₂N + NCH₂P), 4.19 (br. s, 1 H, CH₂C≡CH), 4.14–4.12 (m, 2 H, NCH₂P), 4.11 (br. s, 2 H, CH₂C≡CH) ppm. ³¹P{¹H} NMR ([D₆]DMSO): δ = -51.1 ppm. IR: ν̄ = 2115 cm⁻¹ [ν(C≡C)]. C₁₈H₃₀AuBr₂ClN₆P (784.65): calcd. C 27.55, H 3.85, N 10.71; found C 27.1, H 3.9, N 10.53. S_{25°C}(H₂O): 10.5 g L⁻¹.

Preparation of [AuCl(PTA-R)₂](Cl)₂ Complexes [R = -CH₂CO₂Me (8a), -CH₂Ph (8b)]: [PTA-R]Cl (0.2 mmol) was added to a solution of [AuCl(PTA-R)]Cl (0.2 mmol) in acetone (ca. 10 mL) at 0 °C.

After stirring the mixture for approximately 4 h, the solutions were concentrated and the addition of Et₂O precipitated the products, which were isolated by filtration and dried in air as white solids.

[AuCl(PTA-CH₂CO₂Me)₂](Cl)₂ (8a): Yield 70%, white solid. ¹H NMR ([D₆]DMSO, 25 °C): δ = 5.23 and 5.42 (AB system, *J*_{A,B} = 11.2 Hz, 4 H, NCH₂N), 5.03 (d, *J*_{H,H} = 4.3 Hz, 2 H, PCH₂N), 4.57 (d, *J*_{H,H} = 13.1 Hz, 2 H, NCH₂N), 4.42–4.53 (m, 5 H, PCH₂N + NCH₂N), 4.32 (s, 2 H, CH₂COOMe), 3.75 (s, 3 H, Me) ppm. ³¹P{¹H} NMR ([D₆]DMSO): δ = –24.3 ppm. MALDI MS: *m/z* (%) = : 693 (20) [M]⁺. IR: ν̄ = 1763 cm^{–1} [ν(C=O)]. C₁₈H₃₄AuCl₃N₆O₄P₂ (763.77): calcd. C 28.31, H 4.92, N 11.00; found C 28.33, H 4.74, N 11.27.

[AuCl(PTA-CH₂Ph)₂](Cl)₂ (8b): Yield 72%, white solid. ¹H NMR ([D₆]DMSO, 25 °C): δ = 7.54 (m, 5 H, Ph), 4.92 and 5.13 (AB system, *J*_{A,B} = 11.2 Hz, 4 H, NCH₂N), 4.52 (d, *J*_{H,H} = 13.2 Hz, 1 H, NCH₂N), 4.49 (s, 2 H, NCH₂P), 4.32 (d, *J*_{H,H} = 13.1 Hz, 1 H, NCH₂N), 4.23 (s, 2 H, CH₂Ph), 4.10–4.22 (m, 4 H, NCH₂P) ppm. ³¹P{¹H} NMR ([D₆]DMSO): δ = –49.9 ppm. C₂₆H₃₈AuCl₃N₆P₂ (799.89): calcd. C 39.04, H 4.79, N 10.51; found C 38.75, H 4.56, N 10.27.

Crystallographic Studies: Crystals suitable for X-ray diffraction were obtained by slow diffusion of diethyl ether into methanolic solutions. A summary of the fundamental crystal and refinement data of [PTA-CH₂COOMe]Br (**1a**), [PTA-CH₂Ph]Br (**1b**) and [AuBr(PTA-CH₂Ph)]Br (**5b**) is given in Table 6. The crystals were mounted on a glass fibre with inert oil and centred in a Bruker Smart CCD diffractometer with graphite-monochromated Mo-*K*_α (λ = 0.7107 Å) radiation for data collection. Absorption corrections based on multiple scans were applied by using the SADABS program.^[55] The structures were solved by direct methods^[56] and refined on *F*² by using the SHELXL-97 program.^[57] Hydrogen atoms were included in idealised positions. Weighted *R* factors (*R*_w) and all goodness-of-fit *S* values are based on *F*²; conventional *R* factors (*R*) are based on *F*. The PLATON SQUEEZE^[58,59] algorithm was applied to **5b** to model the diffuse contribution from a

highly disordered solvent of crystallisation to the electron density. CCDC-888587 (for **1a**), -888588 (for **1b**) and -888589 (for **5b**) contain the supplementary crystallographic data for this paper. These data can be obtained free of charge from The Cambridge Crystallographic Data Centre via www.ccdc.cam.ac.uk/data_request/cif.

Antiproliferative Assays: Human A2780 cells were grown in RPMI 1640 medium that contained 10% fetal calf serum (FCS) and L-glutamine (2 mM) under an atmosphere of 5% CO₂ at 37 °C. For the cytotoxicity evaluation, 4000 cells per well were seeded in 100 μL of complete medium in 96-multiwell flat-bottom microtiter plates (Corning Costar). The plates were incubated at 37 °C in 5% CO₂ for 96 h prior to drug testing to allow cell adhesion. Thereafter, a solution (10 μL) of 3-(4,5-dimethyl-2-thiazoyl)-2,5-diphenyltetrazolium bromide [MTT; 5 mg mL^{–1} in phosphate buffer solution (PBS), 0.136 M in NaCl, 1.47 mM in KH₂PO₄, 8 mM in NaH₂PO₄ and 2.68 mM in KCl] were added and incubation was continued for 4 h. Afterwards sodium dodecyl sulfate (SDS) (100 μL; 10% in HCl 0.01 M) was added and incubated for 12–14 h. Then the cell-culture supernatants were removed, the cell layer was dissolved in DMSO, and absorbance at 595 nm was measured in a 96-well multiwell plate reader (Tecan Ultra Evolution) and compared to the values of control cells incubated in the absence of complexes. Experiments were conducted in quadruplicate wells and repeated at least three times. The inhibition of cellular growth was calculated on the basis of the formula: Inhibition [%] = 100 – {(*T* × 100)/*C*} (*T*: observed absorption of the treated cells and *C*: observed absorption in control wells). The inhibitory potency was evaluated by using the concentration versus inhibition [%] of cellular growth curves. These curves were adjusted to the equation *E* = *E*_{max}/[1 + (IC₅₀/*C*)^{*n*}], for which *E* is the percentage inhibition observed, *n* is the slope of the semilogarithmic dose–response sigmoid curves, *E*_{max} is the maximal effect and *C* is the concentration of tested compounds. The nonlinear fitting was performed using GraphPad Prism 2.01, 1996 software. The cytotoxicity of cisplatin was also evaluated under the same experimental conditions for comparison purposes.

Table 6. Crystal data and data collection and refinement for complexes [PTA-CH₂CO₂Me]Br (**1a**), [PTA-CH₂Ph]Br (**1b**) and [AuBr(PTA-CH₂Ph)]Br (**5b**).

	1a	1b	5b
Empirical formula	C ₉ H ₁₇ BrN ₃ O ₃ P	C ₁₄ H ₂₃ BrN ₃ OP	C ₂₆ H ₃₈ Au ₂ Br ₄ N ₆ P ₂
<i>M</i> _r	326.14	360.23	1210.14
Colour, habit	colourless, plate	colourless, irregular block	colourless, plate
Space group	monoclinic, <i>P</i> ₂ /c	monoclinic, <i>P</i> ₂ /c	monoclinic, <i>C</i> 2/c
<i>a</i> [Å]	6.6033(6)	8.3401(13)	23.719(5)
<i>b</i> [Å]	21.9356(18)	11.5736(18)	23.719(5)
<i>c</i> [Å]	9.6615(8)	16.846(3)	16.481(5)
<i>α</i> [°]	90	90	90
<i>β</i> [°]	109.744(2)	96.515(3)	129.963(5)
<i>γ</i> [°]	90	90	90
<i>V</i> [Å ³]	1317.17(19)	1615.6(4)	3358.4(19)
<i>Z</i>	4	4	4
<i>D</i> _{calcd.} [g cm ^{–3}]	1.645	1.481	2.393
<i>μ</i> [mm ^{–1}]	3.243	2.643	13.609
<i>θ</i> range [°]	2.42 to 27.06	2.14 to 27.01	2.13 to 25.00
Data collected	8369	10044	9011
Unique data	2890 [<i>R</i> (int) = 0.0275]	3520 [<i>R</i> (int) = 0.0342]	2961 [<i>R</i> (int) = 0.0399]
<i>R</i> ₁ ^[a] [<i>F</i> ² > 2σ(<i>F</i> ²)]	0.0287	0.0373	0.0442
<i>R</i> ₂ ^[b] (all data)	0.0796	0.0818	0.1300
Largest diff. peak/hole [e Å ^{–3}]	0.656/–0.278	0.577/–0.421	2.719/–2.890
<i>S</i> ^[c] (all data)	1.044	0.906	1.016

[a] *R*₁(*F*) = Σ|*F*_o – |*F*_c||/Σ |*F*_o|. [b] *wR*₂(*F*²) = {Σ[*w*(*F*_o² – *F*_c²)²]/Σ[*w*(*F*_o²)²]}^{1/2}, *w*^{–1} = [σ²(*F*_o²) + (*aP*)² + *bP*], for which *P* = [max(*F*_o², 0) + 2*F*_c²]/3. [c] *S* = {Σ[*w*(*F*_o² – *F*_c²)²]/(n – *p*)^{1/2}}, for which *n* is the number of reflections and *p* the number of refined parameters.

Distribution Coefficients (log $D_{7.4}$): The *n*-octanol/water coefficients of the complexes were determined as previously reported^[60] by using a shake-flask method. PBS-buffered distilled water (100 mL, phosphate buffer [PO₄³⁻] = 10 μM, [NaCl] = 0.15 M, pH 7.4) and *n*-octanol (100 mL) were shaken together for 72 h to allow saturation of both phases. The complexes (1 mg) were mixed in aqueous and organic phase (1 mL), respectively, for 10 min. The resultant emulsion was centrifuged to separate the phases. The concentrations of the compound in each phase were determined by using UV absorbance spectroscopy. The value of log $D_{7.4}$ was defined as [compound_(organic)]/[compound_(aqueous)].

Acknowledgments

We thank the Ministerio de Ciencia e Innovación (MICINN) (grant number CTQ2008-06716-CO3-01) for financial support and Torrecid SA for a generous donation of H[AuCl₄].

- [1] P. Knochel, in: *Modern Solvents in Organic Synthesis* Springer, Berlin, 1999.
- [2] N. Pinault, B. W. Duncan, *Coord. Chem. Rev.* **2003**, *24*, 1–25.
- [3] D. J. Adams, P. J. Dyson, S. J. Tavener, in: *Chemistry in Alternative Reaction Media*, Wiley, Chichester, England, 2004.
- [4] V. I. Siele, *J. Heterocycl. Chem.* **1977**, *14*, 337–339.
- [5] D. J. Daigle, A. B. Peppermann, S. L. Vail, *J. Heterocycl. Chem.* **1974**, *11*, 407–408.
- [6] A. D. Philips, L. Gonsalvi, A. Romerosa, F. Vizza, M. Peruzzini, *Coord. Chem. Rev.* **2004**, *248*, 955–993.
- [7] J. Bravo, S. Bolaño, L. Gonsalvi, M. Peruzzini, *Coord. Chem. Rev.* **2010**, *254*, 555–607.
- [8] D. J. Daigle, A. B. Pepperman Jr., *J. Heterocycl. Chem.* **1975**, *12*, 579–580.
- [9] D. J. Daigle, T. J. Decuir, J. B. Robertson, D. J. Darensbourg, *Inorg. Synth.* **2007**, *32*, 40–45.
- [10] A. Romerosa, T. Campos-Malpartida, C. Lidrissi, M. Saoud, M. Serrano-Ruiz, M. Peruzzini, J. A. Garrido-Cardenas, F. Garcia-Maroto, *Inorg. Chem.* **2006**, *45*, 1289–1298.
- [11] J. M. Forward, R. J. Staples, C. W. Liu, J. P. Fackler, *Acta Crystallogr., Sect. C* **1997**, *53*, 195–197.
- [12] F. P. Pruchnik, P. Smolenski, *Appl. Organomet. Chem.* **1999**, *13*, 829–836.
- [13] J. M. Forward, R. J. Staples, J. P. Fackler, *Z. Kristallogr.* **1996**, *211*, 129–130.
- [14] E. Fluck, J. E. Förster, J. Weidlein, E. Hädicke, *Z. Naturforsch.* **1977**, *32*, 499–506.
- [15] K. J. Fischer, E. C. Aleya, N. Shahnazarian, *Phosphorus Sulfur Silicon Relat. Elem.* **1990**, *48*, 37–40.
- [16] D. A. Krogstad, G. S. Ellis, A. K. Gunderson, A. J. Hamrich, J. W. Rudolf, J. A. Halfen, *Polyhedron* **2007**, *26*, 4093–4100.
- [17] S. Schäfer, W. Frey, A. S. K. Hashmi, V. Cmrecki, A. Luquin, M. Laguna, *Polyhedron* **2010**, *29*, 1925–1932.
- [18] A. Mena-Cruz, P. Lorenzo-Luis, A. Romerosa, M. Saoud, M. Serrano-Ruiz, *Inorg. Chem.* **2007**, *46*, 6120–6128.
- [19] A. Mena-Cruz, P. Lorenzo-Luis, A. Romerosa, M. Serrano-Ruiz, *Inorg. Chem.* **2008**, *47*, 2246–2248.
- [20] A. T. Ekubo, M. R. J. Elsegood, A. J. Lake, M. B. Smith, *Inorg. Chem.* **2009**, *48*, 2633–2638.
- [21] A. S. Humphreys, A. Filipovska, S. J. Berners-Price, G. A. Koutsantonis, B. W. Skelton, A. H. White, *Dalton Trans.* **2007**, 4943–4950.
- [22] A. K. Renfrew, A. E. Egger, R. Scopelliti, C. G. Hartinger, P. J. Dyson, *C. R. Chim.* **2010**, *13*, 1144–1150.
- [23] P. Bergamini, V. Bertolasi, L. Marvelli, A. Canella, R. Gavioli, N. Mantovani, S. Manas, A. Romerosa, *Inorg. Chem.* **2007**, *46*, 4267–4276.
- [24] L. Hajji, C. Saraiba-Bello, A. Romerosa, G. Segovia-Torrente, M. Serrano-Ruiz, P. Bergamini, A. Cannella, *Inorg. Chem.* **2011**, *50*, 873–882.
- [25] S. P. Fricker, *Gold Bull.* **1996**, *29*, 53–60.
- [26] T. M. Simon, D. H. Kunishima, G. J. Vibert, A. Lorber, *Cancer Res.* **1981**, *41*, 94–97.
- [27] C. K. Mirabelli, R. K. Johnson, C.-M. Sung, L. F. Faucette, K. Murihead, S. T. Crooke, *Cancer Res.* **1985**, *45*, 32–39.
- [28] E. Vergara, E. Cerrada, C. Clavel, A. Casini, M. Laguna, *Dalton Trans.* **2011**, *40*, 10927–10935.
- [29] E. Vergara, E. Cerrada, A. Casini, O. Zava, M. Laguna, P. J. Dyson, *Organometallics* **2010**, *29*, 2596–2603.
- [30] E. Vergara, A. Casini, F. Sorrentino, O. Zava, E. Cerrada, M. P. Rigobello, A. Bindoli, M. Laguna, P. J. Dyson, *ChemMedChem* **2010**, *5*, 96–102.
- [31] S. Miranda, E. Vergara, F. Mohr, D. de Vos, E. Cerrada, A. Mendia, M. Laguna, *Inorg. Chem.* **2008**, *47*, 5641–5648.
- [32] L. Maiore, M. A. Cinellu, E. Michelucci, G. Moneti, S. Nobili, I. Landini, E. Mini, A. Guerri, C. Gabbiani, L. Messori, *J. Inorg. Biochem.* **2011**, *105*, 348–355.
- [33] C. Scolaro, A. Bergamo, L. Brescacin, R. Delfino, M. Cocchietto, G. Laurenczy, T. J. Geldbach, G. Sava, P. J. Dyson, *J. Med. Chem.* **2005**, *48*, 4161–4171.
- [34] C. Scolaro, T. J. Geldbach, S. Rochat, A. Dorcier, C. Gossens, A. Bergamo, M. Cocchietto, I. Tavernelli, G. Sava, U. Rothlisberger, P. J. Dyson, *Organometallics* **2006**, *25*, 756–765.
- [35] S. Chatterjee, S. Kundu, A. Bhattacharyya, C. G. Hartinger, P. J. Dyson, *J. Biol. Inorg. Chem.* **2008**, *13*, 1149–1155.
- [36] W. H. Ang, L. J. Parker, A. D. Luca, L. Juillerat-Jeanneret, C. J. Morton, M. L. Bello, M. W. Parker, P. J. Dyson, *Angew. Chem. Int. Ed.* **2009**, *48*, 3854–3857.
- [37] D. J. M. Snelders, A. Casini, F. Edeffe, G. van Koten, R. Gebbink, P. J. Dyson, *J. Organomet. Chem.* **2011**, *696*, 1108–1116.
- [38] C. Rios-Luci, L. G. Leon, A. Mena-Cruz, E. Perez-Roth, P. Lorenzo-Luis, A. Romerosa, J. M. Padron, *Bioorg. Med. Chem. Lett.* **2011**, *21*, 4568–4571.
- [39] P. Nowak-Sliwinska, J. R. van Beijnum, A. Casini, A. A. Nazarov, G. Wagnieres, H. van den Bergh, P. J. Dyson, A. W. Griffioen, *J. Med. Chem.* **2011**, *54*, 3895–3902.
- [40] Z. Assefa, B. G. McBurnett, R. J. Staples, J. P. Fackler Jr, *Inorg. Chem.* **1995**, *34*, 4965–4972.
- [41] Z. Assefa, B. G. McBurnett, R. J. Staples, J. P. Fackler Jr, B. Assmann, K. Angermaier, H. Schmidbaur, *Inorg. Chem.* **1995**, *34*, 75–83.
- [42] E. Fluck, J. E. Forster, J. Weidlein, E. Hädicke, *Z. Naturforsch.* **1977**, *32*, 499–506.
- [43] A. García-Fernández, J. Díez, M. P. Gamasa, E. Lastra, *Inorg. Chem.* **2009**, *48*, 2471–2481.
- [44] L. Hao, M. A. Mansour, R. J. Lachicotte, H. J. Gysling, R. Eisenberg, *Inorg. Chem.* **2000**, *39*, 5520–5529.
- [45] L. Hao, R. J. Lachicotte, H. J. Gysling, R. Eisenberg, *Inorg. Chem.* **1999**, *38*, 4616–4623.
- [46] M. A. Mansour, W. B. Connick, R. J. Lachicotte, H. J. Gysling, R. Eisenberg, *J. Am. Chem. Soc.* **1998**, *120*, 1329–1330.
- [47] C. King, J.-C. Wang, M. N. I. Khan, J. P. Fackler, *Inorg. Chem.* **1989**, *28*, 2145–2149.
- [48] F. Mohr, S. Sanz, E. R. T. Tiekink, M. Laguna, *Organometallics* **2006**, *25*, 3084–3087.
- [49] F. Mohr, E. Cerrada, M. Laguna, *Organometallics* **2006**, *25*, 644–648.
- [50] Z. Assefa, M. A. Omary, B. G. McBurnett, A. A. Mohamed, H. H. Patterson, R. J. Staples, J. P. Fackler, *Inorg. Chem.* **2002**, *41*, 6274–6280.
- [51] E. Vergara, S. Miranda, F. Mohr, E. Cerrada, E. R. T. Tiekink, P. Romero, A. Mendia, M. Laguna, *Eur. J. Inorg. Chem.* **2007**, 2926–2933.
- [52] M. J. McKeage, S. Berners-Price, P. Galettis, R. J. Bowen, W. Brouwer, L. Ding, L. Zhuang, B. C. Baguley, *Cancer Chemother. Pharmacol.* **2000**, *46*, 343–350.

- [53] F. X. Legrand, F. Hapiot, S. Tilloy, A. Guerriero, M. Peruzzini, L. Gonsalvi, E. Monflier, *Appl. Catal. A* **2009**, 362, 62–66.
- [54] C. Papadogianakis, R. A. Sheldon, *New J. Chem.* **1996**, 20, 175–185.
- [55] G. M. Sheldrick, *SADABS, Empirical Absorption Program*, University of Göttingen, Göttingen, Germany, **1996**.
- [56] G. M. Sheldrick, *SHELXS, Program for Crystal Structure Solution*, University of Göttingen, Göttingen, Germany, **1990**.
- [57] G. M. Sheldrick, *SHELXTL-NT*, v. 6.1, *Program for Crystal Structure Refinement*, University of Göttingen, Germany, **1997**.
- [58] P. Vandersluis, A. L. Spek, *Acta Crystallogr., Sect. A* **1990**, 46, 194–201.
- [59] A. L. Spek, *J. Appl. Crystallogr.* **2003**, 36, 7–13.
- [60] C. Wetzel, P. C. Kunz, M. U. Kassak, A. Hamacher, P. Böhrer, W. Watjen, I. Ott, R. Rubbiani, B. Spingler, *Dalton Trans.* **2011**, 40, 9212–9220.

Received: November 21, 2012

Published Online: February 13, 2013